Journal of Hazardous Materials 485 (2025) 136780

Contents lists available at ScienceDirect

Journal of Hazardous Materials

journal homepage: www.elsevier.com/locate/jhazmat

Sensitive and accurate determination of 32 PFAS in human serum using online SPE-UHPLC-HRMS

Masho Hilawie Belay [a,b], Elisa Robotti [a,*], Arianna Ghignone [a], Alessia Fabbris [a], Jessica Brandi [c], Daniela Cecconi [c], Maria Angela Masini [a], Francesco Dondero [a], Emilio Marengo [a]

[a] Department of Sciences and Technological Innovation, University of Piemonte Orientale, Viale Teresa Michel 11, 15121 Alessandria, Italy
[b] Department of Chemistry, Mekelle University, P. O. Box 231, Mekelle, Ethiopia
[c] Department of Biotechnology, University of Verona, Strada le Grazie 15, 37134 Verona, Italy

HIGHLIGHTS

- A sensitive and accurate method for the determination of 32 PFAS in human serum.
- LODs are 5 to 15 times lower than previously reported methods.
- Rinsing protein pellets is critical for improving PFAS recovery.
- MS source regular cleaning is essential to uphold performance and method reliability.

GRAPHICAL ABSTRACT

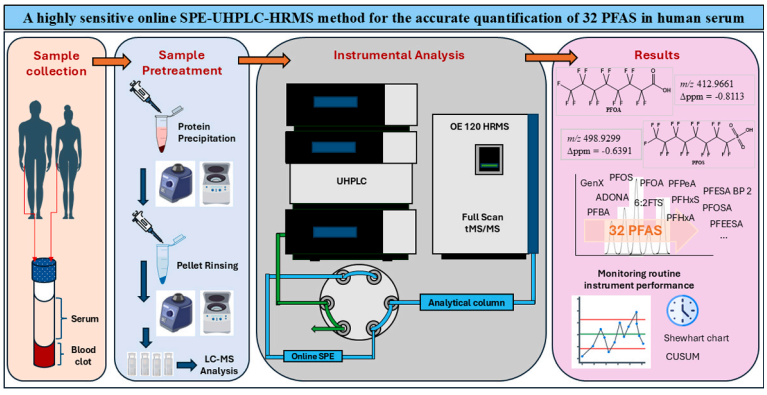

ARTICLE INFO

Keywords:
PFAS
Method development
High resolution mass spectrometry
Human biomonitoring
Serum pretreatment

ABSTRACT

Per- and polyfluoroalkyl substances' (PFAS) extreme persistence has been linked to many adverse effects on human health including increased risk of certain cancers. This study presents the development and validation of a new, highly sensitive method for the quantification of 32 PFAS in human serum using online solid-phase extraction (SPE) coupled with ultra-high performance liquid chromatography–high resolution mass spectrometry (UHPLC–HRMS). Legacy and emerging PFAS were targeted. Main steps of sample pretreatment include protein precipitation (PP), pellet rinsing, centrifugation, preconcentration through solvent evaporation, and online SPE using a weak anion-exchange polymeric sorbent. The PP and pellet-rinsing procedures were optimized through a comprehensive exploration of solvent combinations. Following this, a pretreatment that offers the best compromise for the targeted PFAS was identified using principal component analysis. The method demonstrated excellent linearity ($R^2 = 0.977–0.997$) with limits of quantification ranging from 8.9 to 27 ng/L, 5 to 15 times lower than previous methods. Precision (intraday 2.6–14.0 % and interday 1.3–11.0 % relative standard deviation) and accuracy (recoveries 72.7–106 %) were robust. The method was validated in accordance with ISO/IEC 17025 and successfully applied to five human serum samples, confirming its suitability for high-

* Corresponding author.
E-mail address: elisa.robotti@uniupo.it (E. Robotti).

https://doi.org/10.1016/j.jhazmat.2024.136780
Received 1 September 2024; Received in revised form 2 December 2024; Accepted 3 December 2024
Available online 4 December 2024

throughput profiling of PFAS in biomonitoring studies. This method is the first to use online SPE for the simultaneous determination of a broad range of PFAS, including ether congeners such as perfluoro(2-ethoxyethane) sulfonic acid and Nafion byproduct 2. Furthermore, control charts were employed to assess instrument performance during routine analysis and implement necessary actions.

1. Introduction

Per- and polyfluoroalkyl substances (PFAS) are a large class of synthetic chemicals considered important emerging contaminants [1]. These substances are used globally across a wide range of industrial and consumer products. Over the past 50 years, PFAS have been incorporated into the production of surfactants, lubricants, paints, varnishes, food packaging, fire-retardant foams, cosmetics and personal care products, and insecticides, and are extensively used in sectors such as the automotive, aerospace, chemical, electrical, medical, and construction industries [2]. PFAS are generally characterized by a linear or branched hydrophobic carbon chain, which can be partially or fully fluorinated, and a terminal hydrophilic group. Depending on the type of charge carried by the terminal hydrophilic group, these substances can exist in cationic, anionic, or neutral forms. The strong carbon–fluorine bonds confer exceptional resistance to heat, pH, thermal degradation, biodegradation, hydrolysis, and metabolism, resulting in their high persistence in the environment. Consequently, PFAS are classified as persistent organic pollutants (POPs) [3,4]. Owing to their unique physicochemical properties, persistence, and mobility, PFAS have been detected at trace levels across various environmental matrices and biological tissues, including water [5–8]; human serum and plasma [9,10]; breast milk [11]; air [12]; marine organisms such as fish, reptiles, birds and mammals [13]; and food and feed [14].

Currently, over 9000 compounds are categorized under the PFAS class [15], encompassing both legacy and emerging substances. The term “legacy PFAS” refers primarily to long-chain perfluorosulfonic acids (PFSAs) and perfluorocarboxylic acids (PFCAs) [3], the most prominent of which are perfluorooctanesulfonic acid (PFOS) and perfluorooctanoic acid (PFOA), which are detected almost ubiquitously in the environment and biota [15]. Short-chain PFAS, also known as “emerging PFAS”, have been adopted by the chemical industry as alternatives to long-chain PFAS. However, these emerging PFAS are now being increasingly detected in the environment and in humans at significant levels, due to their unrestricted use [16,17]. One of the most important examples of an emerging PFAS is HFPO-DA (hexafluoropropylene oxide – dimer acid), also known as GenX, which is a replacement for PFOA in many industrial applications including fluoropolymer resins and plastics [18].

International concern about the health effects of PFAS exposure first began in the early 2000s following the detection of PFOS and PFOA in wildlife from remote regions [2]. Over the last decade, significant progress has been made in understanding the adverse effects of these substances on human health, leading to the introduction of regulatory measures. Concurrently, the chemical industry has shifted towards short-chain PFASs as alternatives; however, several studies suggest that these emerging PFAS may pose similar health risks [15,19]. Today, PFAS are prevalent worldwide, impacting both wildlife and humans, with dietary intake from food and drinking water identified as the primary route of human exposure [20].

PFAS have the potential to cause various adverse health effects influenced by the extent, duration, and route of exposure as well as individual and genetic predisposition. Recent scientific studies [15] confirmed that exposure to certain levels of PFAS can lead to reduced fertility, immune and endocrine effects, delays in children’s development and growth, and increased risk of various cancers, including prostate, renal, and testicular cancers [1,6,15,21–23]. Furthermore, the International Agency for Research on Cancer (IARC) has classified PFOA as a Group 1 human carcinogen, indicating it is carcinogenic to humans, while PFOS has been classified as a Group 2B carcinogen [22].

The most straightforward and rapid assessment of PFAS contamination in humans is through blood serum analysis, as it directly reflects the ongoing accumulation within the body [14,24]. Various human biomonitoring studies have revealed vital information on the trends of serum PFAS. A European human biomonitoring initiative [25] carried out among 1957 European teenagers aged 12–18 analyzed four PFAS (PFOS, PFOA, perfluorononanoic acid [PFNA], and perfluorohexanoic acid [PFHxS]), revealing that serum PFAS levels in 14.3 % of the teenagers surpassed the European Food Safety Authority’s tolerable weekly intake value of 6.9 μg/L PFAS. The main sources of exposure identified were drinking water and foods such as fish, eggs, and offal. This study also reiterated the importance of monitoring PFAS exposure in specific workplaces due to the very high levels of PFAS exposure found in workers. Pitter et al. (2020) [26] studied 18,345 people aged 14–39 in the Veneto region of Italy and found elevated serum PFAS levels, including PFOA (median, 44.4 μg/L), PFHxS (3.9 μg/L), and PFOS (3.9 μg/L). A worldwide probabilistic assessment [27] of serum PFAS levels and risk profile evaluated PFOS, PFOA, PFNA, and PFHxS in pregnant women and children. The study revealed that PFOS was prevalent in the serum and that PFAS exposure has implications for infant development and immune effects. In a study conducted on the United States population [28], perfluorodecanoic acid (PFDA), PFHxS, PFNA, PFOS, and PFOA were frequently detected; however, their levels generally declined from 1999 to 2018. The frequent and high PFAS exposure documented by various studies emphasizes the need for continuous PFAS human biomonitoring. Studies (e.g., [28]) have further shown that current methods and technologies are incapable of detecting some PFAS in biological samples at extremely low levels, emphasizing the need for advanced methods and technologies.

Among the techniques used for extracting and preconcentrating PFAS from serum samples, online solid phase extraction (SPE) has gained popularity over the past decade due to its ability to provide good reproducibility, rapid analysis, efficient clean-up from interferents, and reduced sample contamination compared with the offline SPE methods [24,29]. High performance liquid chromatography coupled with tandem mass spectrometry (HPLC–MS/MS) is the most commonly used technique for determining trace levels of non-volatile PFAS in serum [30]. Recent advancements in mass spectrometry have enabled the use of high-resolution mass spectrometry (HRMS) for PFAS detection, allowing for the differentiation of accurate masses of analytes with extremely high precision and sensitivity [24].

Quantifying PFAS at trace levels requires efficient extraction and clean-up procedures to enrich samples and minimize matrix interferences [12]. Recently, methods combining online SPE with LC–HRMS have increasingly been used to measure emerging contaminants in environmental and human samples. Online SPE automates the sample clean-up and analyte enrichment processes, effectively addressing challenges related to processing time and contamination within laboratory workflow [31]. For example, Kato et al. (2018) [32] used an online SPE and HPLC-MS/MS method to determine 18 perfluorinated compounds in serum and urine. Similarly, Poothong et al. (2017) [33] combined online SPE and UHPLC–MS/MS to develop a sensitive method for simultaneously determining 25 PFAS in human serum, plasma, and whole blood. Liu et al. (2019) [34] also reported several methods using online SPE and HRMS to determine PFAS in different samples, including water, soil, air, and serum. However, all of these methods share a common obstacle: developing a highly sensitive method for the simultaneous determination of multiple PFAS classes

remains challenging due to the diverse physicochemical properties of these compounds. Consequently, any final optimized method usually represents the best compromise for their simultaneous determination.

In light of the aforementioned challenges, this study's objectives and original contributions are outlined as follows. (1) To develop an online SPE–UHPLC–HRMS method for the simultaneous determination of 32 PFAS in human serum, including both legacy and emerging compounds. While previous studies on online SPE have focused on a limited number of PFAS [12,35,36], we expanded the scope of research in this study by including several emerging fluoroalkylether congeners (ether-PFAS), such as perfluoro(2-ethoxyethane)sulfonic acid (PFEESA), Nafion byproduct 2 (PFESA BP 2), hexafluoropropylene oxide dimer acid (HFPO-DA or GenX), and dodecafluoro-3H-4,8-dioxanonanoate (ADONA). (2) To investigate various protein precipitation (PP) and pellet rinsing methods to optimize PFAS recovery from human serum. Extensive literature exists on the application and effects of PP in PFAS extraction from human serum. However, to our knowledge, this study presents the first comprehensive analysis of the effect of rinsing protein pellets on PFAS recovery. Following pellet rinsing, all targeted PFAS recoveries showed significant improvement. Therefore, we highly recommend integrating this procedure into serum PFAS analysis to avoid underestimating concentrations due to insufficient recoveries. (3) This new analytical method offers detection limits that are 5 to 15 times more sensitive than those in previous studies. This greatly facilitates the accurate determination of trace-level serum PFAS concentrations, supporting biomonitoring efforts in human populations.

2. Materials and methods

2.1. Chemicals

Water, methanol, acetonitrile, and formic acid were all LC-MS grade (purity ≥99.9 %) purchased from VWR International (Milan, Italy); ammonium acetate (≥99.9 %) was from Sigma-Aldrich (Milan, Italy). A total of thirty-two PFAS congeners were targeted in this study, of which 30 individual native standards and a mixture of 24 isotopically labeled internal standards (ILIS; MPFAC-HIF-ES) were purchased from Wellington Laboratories (Guelph, Ontario, Canada). Two native PFAS standards were from Apollo Scientific (Bredbury, Stockport, UK). Target PFAS included C_4–C_{14} perfluoroalkyl carboxylic acids (PFCAs), C_4–C_{10} and C_{12} perfluoroalkyl sulfonic acids (PFSAs), PFAS precursors/replacements including (N-alkyl substituted) perfluorooctane sulfonamide/acetate (FOSAs and FOSAAs), fluorotelomer sulfonates (FTSs), and emerging fluoroalkyl ether substances HFPO-DA (GenX), ADONA, PFEESA, and Nafion byproduct 2 (PFESA BP2). See Table S1 (Supplementary Information) for the complete list of the native and mass-labeled standards. An additional six PFAS were included in the initial method target lists but were omitted from the final method due to unacceptable method performance. The compounds were 2H-perfluoro-2-octenoic acid (6:2FTUA), 2H-perfluoro-2-decenoic acid (8:2FTUA), 2H-perfluoro-2-dodecenoic acid (10:2FTUA), 6:6 perfluoroalkylphosphinic acid (6:6PFPiA), 6:8 perfluoroalkylphosphinic acid (6:8PFPiA), and 8:8 perfluoroalkylphosphinic acid (8:8PFPiA).

2.2. Preparation of standard solutions

A 1.0 μg/mL stock solution of all 32 native PFAS, prepared in methanol, was used to create diluted solutions for calibration curves and spiking experiments. The stock solutions were stored frozen at −20 °C and thawed overnight in a refrigerator before being brought to room temperature on the day of use. Working solutions were stored in a refrigerator for up to one week. Calibration standards, quality controls, and spiking solutions were freshly prepared each day. Unless stated otherwise, calibration standards, quality controls, blanks, and serum samples were prepared in methanol/water (20:80, v/v) for injection into the LC–MS system.

2.3. Protein precipitation and PFAS extraction

We analyzed various unknown samples (human pooled serum) in search of a blank matrix with a low PFAS level. However, none of the tested sera were suitable for use, due to the very high levels of perfluorooctanoic acid (PFOA), perfluorooctanesulfonic acid (PFOS), and perfluorohexanesulfonic acid (PFHxS) present in all the tested samples. Consequently, method development and validation were carried out using matrix-matched newborn calf serum obtained from Capricorn Scientific GmbH (Ebsdorfergrund, Germany), which contained relatively lower background levels of PFOA (14.7 ng/L) and PFOS (22.4 ng/L).

Protein precipitation (PP) procedures with pure or acidified (0.1 % formic acid) acetonitrile and methanol were investigated. The extraction of PFAS bound to the protein pellet was also examined by rinsing the pellet with the solvents used for PP. An overview of the procedure is depicted in Fig. 1 (see also Fig. S1 in the Supplementary Information for more details).

In the final optimized method, the best conditions for extracting the target PFAS were as follows: 80 μL of serum sample was transferred into a 1.5-mL polypropylene centrifuge tube, followed by the addition of 10 μL of internal standard and 300 μL of acetonitrile containing 0.1 % (v/v) formic acid. The contents were gently vortexed for 60 s and then centrifuged at 13,500 rpm at 4 °C for 10 min. Next, the supernatant was transferred to a new polypropylene centrifuge tube and the original tube containing the pellet was further rinsed with 300 μL methanol, vortexed, and centrifuged at 13,500 rpm at 4 °C for 10 min. The supernatant from the second centrifugation was combined with the first, and the mixture was dried in a SpeedVac Concentrator at 30 °C (Concentrator 5301, Eppendorf, Germany). The samples were reconstituted with 100 μL of methanol and diluted 1:10 (v/v) with methanol/water (20:80, v/v) before analysis.

To develop the standard addition curve with four levels, including the zero-point, three pooled serum extract replicates were prepared as follows: a) nine serum samples were separately pretreated and reconstituted (100 μL each) after SpeedVac evaporation; b) three pooled replicates were created by combining three samples into a single microcentrifuge tube; c) each pooled replicate was divided into four 50-μL aliquots (twelve samples total, representing three samples for each standard addition level), and then 10 μL of the isotopically labeled internal standards (ILIS) was added to each aliquot; d) three of the aliquots were fortified with 10 μL of PFAS standards containing increasing amounts of the target analytes (final in-vial concentrations of 20.0, 40.0, and 60.0 ng/L), while one aliquot was analyzed as is (considered as the zero-point) by adding 10 μL of methanol; e) all four aliquots were adjusted to 350 μL by adding LC–MS water and then subjected to online SPE pretreatment before being analyzed using UHPLC-HRMS.

2.4. Online solid-phase extraction (SPE) method

A Thermo Scientific Dionex UltiMate 3000 UHPLC System (Thermo Scientific, Waltham, MA, USA) equipped with dual gradient pumps (DGP-3600SD), a solvent rack (SRD-3600) with six degasser lines, a thermostated analytical autosampler (WPS-3600TSL), and a thermostated column compartment (TCC-3000SD) was used. A Viper Online SPE Kit was employed to connect a 2-position, 6-port switching valve with the UHPLC system and automate the online SPE sample pretreatment before UHPLC separation. During method development, two online SPE cartridges were investigated: a Hypersil Gold C18 (20 × 2.1 mm, 12 μm; Thermo Scientific, Waltham, MA, USA) and a weak anion-exchange Strata-X-AW online SPE cartridge (20 × 2.0 mm, 25 μm; Phenomenex, Bologna, Italy). In the final method, the Strata-X-AW online SPE cartridge was selected for use with the loading pump. The online SPE follows the same fundamental principles as liquid chromatography (LC), as discussed elsewhere [26]. In brief, a mobile phase from the loading pump (left pump) delivers the sample into a

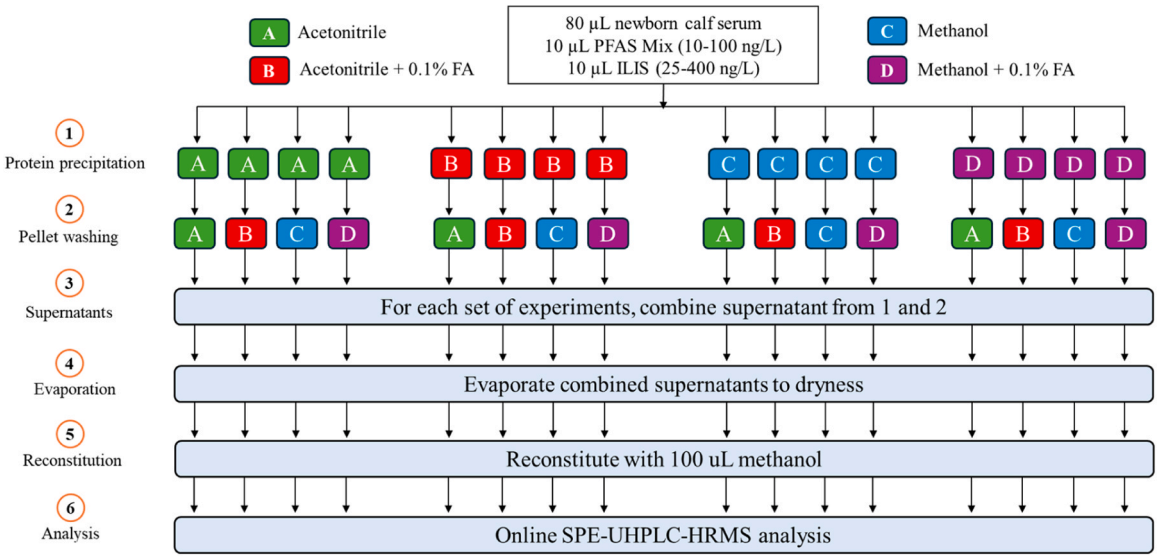

Fig. 1. : Overview of the serum protein precipitation and pellet rinsing experiments performed using various solvent combinations.

pre-conditioned online SPE column for 3.0 min at 2.0 mL/min flow rate. The target analytes are retained on the SPE sorbent (enrichment), while interferences are removed to waste (clean-up). Simultaneously, the analytical column is equilibrated using the eluting pump (Fig. 2a). This setup enables the injection of significantly larger sample volumes than standard HPLC systems. After sample loading and rinsing, a valve switches to connect the eluting pump to the SPE column. The mobile phase from the eluting pump, which is also used for the chromatographic separation, elutes the compounds from the online SPE column and delivers them into the analytical column (Fig. 2b), where they are separated and detected by Orbitrap HRMS. During the final stages of the HPLC separation (10.5 min), a valve switch is triggered to revert to the configuration depicted in Fig. 2a, allowing for simultaneous online SPE column preparation for the next injection while the HPLC separation is still in progress (additional details in Table 1).

2.5. UHPLC-HRMS analysis

All analyses were performed using a Dionex 3000 UHPLC system coupled with an Orbitrap Exploris 120 high-resolution mass spectrometer (HRMS), both from Thermo Scientific (Waltham, MA, USA). The Orbitrap Exploris 120 was equipped with an OptaMax NG ion source housing consisting of a heated-electrospray ionization (HESI-II) interface and a Chemyx SKE10 syringe pump. The HPLC autosampler was configured with a viper injection kit consisting of a 500-µL syringe and 667-µL sample loop. The HPLC loading pump was dedicated to

Table 1
Online SPE and UHPLC gradient conditions.

Online SPE (Loading pump)					**UHPLC (Eluting pump)**		
A: Water B: Methanol C: Methanol/Acetonitrile (50:50, v/v)					A: 5 mM Ammonium acetate B: Methanol/Acetonitrile (50:50, v/v)		
Time (min)	%A	%B	%C	Flow (mL/min)	Time (min)	%B	Flow (mL/min)
0.00	100	0	0	2.0	0.00	10	0.3
3.00	100	0	0	2.0	2.00	10	0.3
3.01	0	100	0	1.5	3.00	45	0.3
6.00	0	100	0	1.5	6.00	95	0.3
6.01	0	0	100	1.0	11.30	95	0.3
10.49	0	0	100	1.0	11.31	10	0.3
10.50	0	100	0	2.0	15.00	10	0.3
12.75	0	100	0	2.0			
12.76	100	0	0	2.0			
15.00	100	0	0	2.0			

Switching valve positions:
- 0.0 min: Loading pump to SPE column; eluting pump direct to analytical column.
- 3.0 min: Loading pump to waste; eluting pump to SPE and onto analytical column.
- 10.5 min: Loading pump to SPE column; eluting pump direct to analytical column.

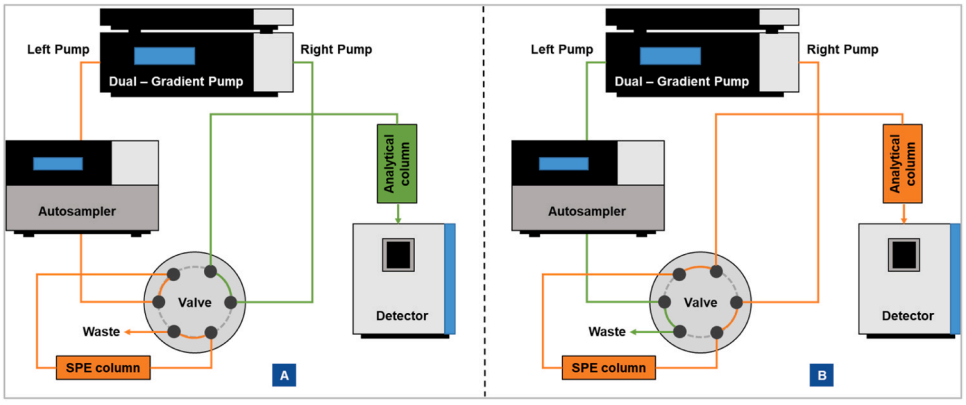

Fig. 2. Configuration of the online SPE and valve switching system: sample loading on the SPE cartridge (A); elution of the analytes from the cartridge to the column (B).

automated sample preparation with online SPE, while the eluting pump was used to separate target analytes with a chromatographic column. Three reversed–phase columns were evaluated for chromatographic separation: the Acclaim RSLC 120 C18 (2.1 × 100 mm, 2.2 μm; Thermo Scientific, Waltham, MA, USA), the Kinetex C18 (2.1 × 100 mm, 2.6 μm; Phenomenex, Bologna, Italy), and the Luna Omega PS C18 column (2.1 × 100 mm, 1.6 μm; Phenomenex, Bologna, Italy). Parameters such as retention time stability, peak shape, and resolution were evaluated, and all columns gave good performance for long chain PFAS (C > 8). However, the Luna Omega PS C18 column exhibited superior performance for short chain congeners (C4–C6; more discussion is provided in the Results and Discussion section). Consequently, the final method uses the Luna Omega PS C18 column. The mobile phase consisted of 5 mM ammonium acetate and methanol/acetonitrile (1:1, v/v), eluting under the gradient conditions shown in Table 1. The autosampler and column temperatures were 10 and 40 °C, respectively. The injection volume was 200 μL. The chromatographic separation time was 11.3 min, giving a total chromatographic cycle time of 15 min including pre-injection equilibration.

In the Orbitrap, a heated electrospray ionization (H-ESI) source with negative ionization was used, and the MS data were acquired with a combination of Full Scan (FS) and targeted MS/MS scans (tMS^2), as detailed in Table 2. Dynamic exclusion and mass list parameters with 2 ppm mass tolerance were used to define the tMS^2 triggering algorithm. The most intense precursor ions obtained from the high-resolution accurate mass (HRAM) data acquired in FS at 120,000 resolution (*m/z* 200) were used as quantifier ions. For all target analytes, the $[M\text{-}H]^-$ ions were the most intense precursor masses, except for GenX, where the in-source fragment $[M\text{-}CO_2\text{-}H]^-$ was the most intense precursor ion. For each analyte, at least one HRAM fragment ion with a mass error less than 5 ppm was monitored as a qualifier ion in the tMS/MS. The complete list of quantifier and qualifier ions is provided in Table S2 (Supplementary Information).

2.6. Quality assurance and quality control

Polypropylene labware pre-cleaned with LC/MS-grade methanol was used throughout method development and validation. In spiking sample aliquots with PFAS standards, the standard practices of quality control were followed to ensure minimal loss of analyte during preparation. The vials, microcentrifuge tubes, and pipette tips used were made of low retention virgin polypropylene. Micropipettes were regularly cleaned and calibrated according to manufacturer guidelines. Working standard solutions were prepared freshly on the day of experimentation. To minimize variability due to the formation of a film in the liquid, pipette tips were pre-washed with the standard solution twice before the desired volume was measured. Then, the blank sample in a microcentrifuge tube was immediately spiked with the standard solution, and the pipette tip was washed three times with the sample in the microcentrifuge tube to ensure the complete transfer of the volume measured.

Ultra-high purity mobile phases were employed, and any PFAS potentially introduced upstream of the injector were temporarily trapped in a delay column installed before the injector to prevent coelution with the sample analytes. LC-MS water spiked with mass-labeled internal standards was run as a procedural blank in each batch of samples. Carryover effects were monitored by analyzing a solvent blank after the highest concentration standard in the calibration curve, and no carryover was detected for any target analytes. The Orbitrap was routinely calibrated using the Thermo Scientific Pierce FlexMix calibration solution to ensure data quality (HRAM with mass error < 2 ppm). During sample analysis, the mass was calibrated before each sample injection using the internal calibrant RunStart EASY-IC system.

The target compounds were quantified using the isotope dilution method, applying external calibration, or using the standard addition method (SAM) [37]. For target compounds lacking mass-labeled analogues, a structurally similar ILIS with a close retention time was used (see Table S1, Supplementary Information). When serum samples were diluted 1:100, the matrix effect was not significant, allowing for six-point calibration curves in the range of 1–500 ng/L ($R^2 > 0.997$) to be prepared in methanol/water (20:80, v/v) for each analyte, with internal standards at a constant concentration. For serum samples diluted 1:10, significant matrix effects were observed, so four-point SAM measurements were used to calculate the regression equations ($R^2 > 0.997$ for all analytes). Limits of detection (LODs) and limits of quantification (LOQs) were calculated from the calibration curves using the Hubaux-Vos method [38] and the method recommended by the International Committee on Harmonization (ICH) [39]. Matrix-spiked precisions and recoveries were also evaluated and are discussed below in the *Results and Discussion* section. The LC–MS performance was monitored over time using Shewhart's and Cumulative Sums (CUSUM) control charts for potential environmental or equipment effects. This approach allowed us to assess the instrument's performance and identify when intervention, such as cleaning the ESI source, was necessary. Shewhart's control charts [40] were used to monitor the slope of the standard addition method (SAM) over time, with control limits set at ± 20 % matrix effect. Additionally, CUSUM charts [41] were employed to detect subtle changes that might not be captured by Shewhart's charts.

Table 2
Orbitrap mass spectrometry parameters used for PFAS analysis.

HESI-II ion source properties			
Ionization mode	H-ESI negative	Sweep gas (Arb)	1.0
Spray voltage (| kV|)	1.5	Ion transfer tube temp. (°C)	270
Sheath gas (Arb)	30	Vaporizer temp. (°C)	300
Aux gas (Arb)	10		
Full Scan (FS) MS		**Targeted MS/MS (tMS^2)**	
Orbitrap resolution	120,000	Orbitrap resolution	15,000
Scan rang (*m/z*)	100 −1000	Isolation window (*m/z*)	1.2
RF lens (%)	70	HCD collision energies (V)	15, 30, 60
AGC target	1×10^6	Collision energy type	Normalized
Max. injection time mode	Auto	AGC target	2×10^5
Microscan	1.0	Max. injection time mode	Auto
MS divert valve:	0 −5 min to waste; 5 −11 min to MS; 11 −15 min to waste		

2.7. Method application

The validated method was applied to human serum samples collected on August 2, 2024, from five individuals, all of whom were co-authors of this study. Each participant provided informed consent, and the five samples were treated anonymously. First, the collected blood samples were allowed to clot by leaving them undisturbed for 25 min at room temperature. The samples were then centrifuged at 2000 × g for 10 min in a refrigerated centrifuge. The resulting supernatants, identified as serum, were then transferred to clean polypropylene tubes. The serum samples were subsequently processed according to the methods outlined in Section 3.1 – Method Development; this involved PP followed by online solid-phase extraction (SPE) ultra-high-performance liquid chromatography (UHPLC) high-resolution mass spectrometry (HRMS) analysis.

2.8. Software

LC-HRMS data acquisition and processing were performed using TraceFinder 5.2 software (Thermo Scientific, Waltham, MA, USA). Principal component analysis (PCA) was performed with Statistica v.7 (Statsoft Inc, Tulsa, OK, USA). Shewhart's and CUSUM control charts were created using Microsoft Excel 2016 (Microsoft Corporation, Redmond, WA, USA). Graphical representations were also generated using

Statistica v.7 and Microsoft Excel 2016.

3. Results and discussion

3.1. Method development

The low concentrations of PFAS in biological samples have driven the demand for highly sensitive LC-MS/MS methods capable of quantifying trace levels with high precision and accuracy, which necessitate meticulous optimization of sample preparation. Therefore, method development and validation are crucial for ensuring accurate, precise, and reliable analyte identification and quantification [42]. PFAS analysis in serum is particularly challenging due to the often limited sample volume, the complex matrix, and potential matrix interferences, especially for short-chain congeners such as perfluorobutanoic acid (PFBA) and perfluoropentanoic acid (PFPeA) [43]. Most serum PFAS methods in the literature rely on a single-step PP using solvents like acetonitrile or methanol [44]. However, multiple studies have shown that both short-chain and long-chain PFAS can preferentially bind proteins [45, 46], and single-step extractions may not quantitatively release protein-bound PFAS. Human serum is composed of 75–82 % water, 5.8–8.6 % protein, 0.45–1.2 % fat, 0.19–0.64 % fatty acids, and 0.56–0.62 % inorganic salts [47]. If matrix components (proteins, lipids, and inorganic salts) are not efficiently removed during sample preparation, matrix effects could compromise measurement accuracy. Therefore, various PP methods and online SPE procedures were systematically tested to achieve optimal PFAS extraction and sample clean-up, as detailed in the following sections.

3.1.1. Protein precipitation

Different solvents were investigated for PP and the recovery of protein-bound PFAS, as shown in Fig. 1. Prior to evaluating the performance of various solvent combinations, the significance of rinsing the pellet after PP was thoroughly examined using serum samples spiked with ILIS at concentrations ranging from 25 to 400 ng/L. The results presented in Fig. 3 show that rinsing the pellet significantly improved PFAS recovery (see additional graphs in Supplementary Information, Fig. S2). Relative peak areas increased across all compounds, with

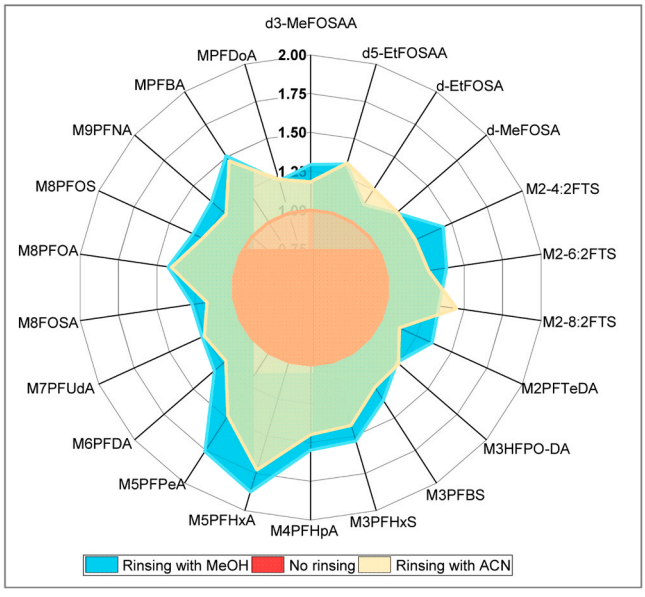

Fig. 3. Effect of protein pellet rinsing methods on PFAS recovery. Radar chart comparing PFAS recovery from serum samples using no rinsing (red/orange), methanol rinsing (MeOH, blue), and acetonitrile rinsing (ACN, yellow). Results are presented as ratios relative to single-step serum precipitation without rinsing.

acetonitrile precipitation followed by methanol rinsing providing the best results. Compared with the commonly used single-step PP (red/orange), peak areas increased from 13 % (M2PFTeDA) to 87 % (M5PFHxA) after methanol rinsing (blue), and by 17 % (M8FOSA) to 73 % (M5PFHxA) with acetonitrile rinsing (yellow). Short-chain perfluorocarboxylic acids and perfluorosulfonates (C4–C7) exhibited significantly greater improvements than did the long-chain congeners (C8–C14).

Considering the overall improvement in the peak areas of the internal standards due to rinsing, it was necessary to determine whether similar benefits could be achieved for native PFAS. Serum was spiked with a PFAS mix containing all target PFAS at 50 ng/L, and proteins were precipitated using acetonitrile (A) or acetonitrile with 0.1 % formic acid (B). The rinsing stage involved five different rinsing solvents: acetonitrile (A), methanol (B), 1:1 acetonitrile/methanol (C), 1:3 acetonitrile/methanol (D), and 3:1 acetonitrile/methanol (E). The experiments were carried out in duplicate. The peak area ratios (native PFAS divided by internal standard) and coefficients of variation (%CV) were assessed through PCA, with results shown in Fig. 4. The samples were labeled with a three-character code in the score plots: the first letter refers to the PP method (A or B), the second letter to the rinsing solvent (A to E), and the number to the replicate (1 or 2).

For the ratios, most PFAS exhibited negative loadings on PC1 (Fig. 4b), indicating that samples with negative scores in the score plot (Fig. 4a) yielded larger peak areas and better results. The AB, AC, BD, and BB combinations appeared to provide the most consistent results. However, the AA combination showed greater variability between the two replicates, suggesting that its reproducibility may be less reliable. Among the better-performing combinations, BD and BB (with positive scores on PC2) yielded larger ratios for PFPeS, PFEESA, PFOS, and PFDA, while AB and AC (with negative scores on PC2) were more effective for PFDS, PFNS, GenX, and PFTrDA.

Regarding the %CV, most molecules had positive loadings on PC1 (Fig. 4d), meaning that conditions with the smaller %CV values corresponded to negative scores in the score plot (Fig. 4c). The best repeatability was achieved using acidified acetonitrile for PP, with the BB and BE combinations yielding the most consistent results.

Precipitation with acidified acetonitrile (0.1 % formic acid) followed by methanol rinsing (option BB in Fig. 4) was identified as the most effective compromise for all targeted PFAS. To evaluate the impact of multiple rinsing steps, the protein pellet was rinsed with methanol five times, with the supernatant from each stage collected into a new centrifuge tube. The peak areas from the five rinsing phases (W1–W5) were compared with those from single-step PP (W0). Only six PFAS (MeFOSAA, EtFOSAA, EtFOSA, MeFOSA, PFBA, and PFHxS) showed slight improvements at W2 (see Fig. S3 in the Supplementary Information). However, the increases were all less than 5 % compared with W1. Consequently, the final optimized method included only one rinsing step.

Studies have shown that PFAS binding to serum proteins affects their accumulation, circulation, and elimination in humans [46]. This indicates that PFAS binding to serum proteins may compromise extraction efficiency when using a simple PP method, such as acetonitrile. The literature provides limited information on the impact of rinsing the protein pellet on PFAS extraction, with only a few studies mentioning this additional step (e.g., [48]). We found that rinsing the protein pellet was crucial to improving PFAS recoveries and incorporated this step into the analytical method workflow.

3.1.2. The online SPE method

PFAS analysis in serum often involves a single-step sample preparation procedure, such as PP or SPE. However, these approaches alone may not remove all the matrix components, complicating analytical method validation and affecting performance. As a result, a multistep sample preparation procedure (PP followed by SPE) has become increasingly popular [48]. Furthermore, when analyzing large numbers

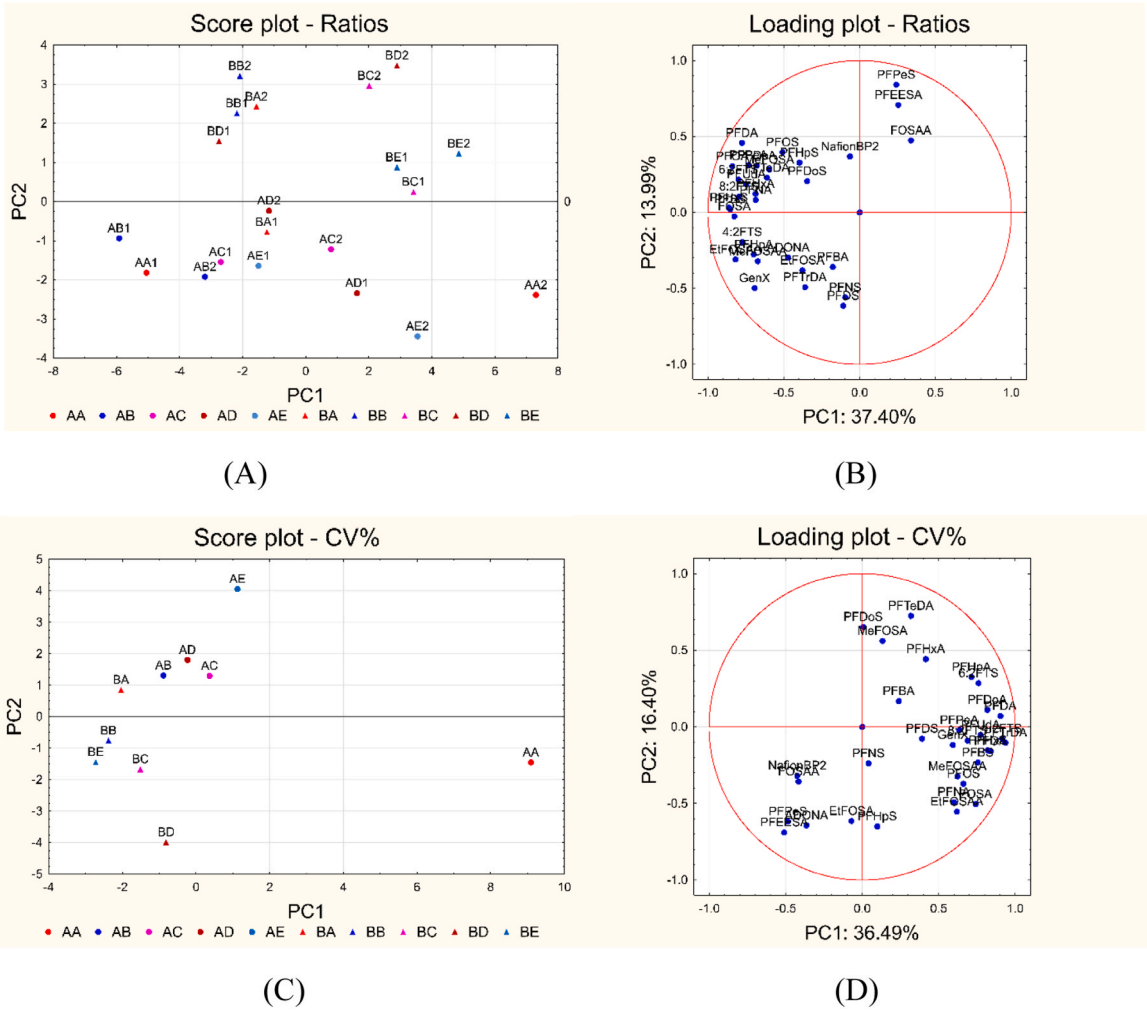

Fig. 4. PCA analysis of PFAS signal ratios and repeatability (%CV) across different precipitation and rinsing conditions. Results of PCA applied to signal ratios (score plot A and loading plot B); % CV values (score plot C and loading plot D). The total variance explained by PC1 and PC2 was approximately 53 %. A three-character label is used for the samples in the score plot of ratios: the first letter refers to the PP (A = acetonitrile; B = acetonitrile + 0.1 % formic acid); the second letter to the rinsing step (A = acetonitrile, B = methanol, C = 1:1 acetonitrile:methanol, D = 1:3 acetonitrile:methanol, E = 3:1 acetonitrile:methanol), and to the replicate number (1 or 2).

of serum samples, frequent maintenance of the analytical instrument is required (e.g., changing the pre-column more frequently and cleaning the ESI source). A multistep sample preparation method may produce cleaner extracts, reducing the need for equipment maintenance. Online SPE, as opposed to offline SPE, needs minimal or no sample pretreatment. This improves repeatability and sensitivity and decreases contamination risks while providing low LODs and LOQs.

In light of these benefits, the serum obtained after PP was further purified with online SPE. The two most common sorbents used in serum PFAS analysis were tested: a weak anion exchange (WAX) with hydrophobic and anion-exchange characteristics and the standard C18 cartridge. The WAX sorbent provided enhanced ionization in ESI-negative mode for majority of the target analytes and internal standards (data shown in Fig. S8 of the Supplementary Information). WAX-based SPE purification for serum PFAS analysis typically showed notable ionization enhancement. This was due to reduced matrix interference resulting from improved extraction and clean-up [49], which aligns with our findings. Indeed, the strong affinity and reversible interactions of the WAX sorbent with PFAS [50] could account for its enhanced performance as most of the target analytes have acidic moieties like carboxylic and sulfonic acids.

Various loading and elution conditions were tested to confirm that ion exchange was the dominant mechanism over hydrophobic interactions. For online SPE, water with or without 0.1 % formic acid was tested as the loading mobile phase. The elution solvents were those used for chromatographic separation, and we tested water containing 2, 5, or 10 mM ammonium acetate (A) and acetonitrile/methanol 1:1 (B). Data related to these tests are provided in the Supplementary Information (Figs. S10 and S11). The results indicate that the interactions between most analytes and the online SPE sorbent were primarily ionic, meaning anionic exchange was dominant over the reversed-phase mechanism. Therefore, the final method uses the Phenomenex Strata-X-AW online SPE column, which is the most commonly used sorbent in studies involving serum purification for PFAS analysis [47,51]. With the weak-anion exchange sorbent, very good recoveries were obtained for PFBA and PFPeA— the two most challenging short-chain PFAS. All analytes were eluted from the SPE using a mobile phase mixture of 5 mM ammonium acetate in water and methanol/acetonitrile (1:1, v/v). The presence of acetonitrile in the mobile phase was essential for minimizing reversed-phase interactions between the analytes and the analytical separation column and resulted in improved chromatographic peak shapes. Automating the SPE procedure online with the HPLC system offered advantages such as a smaller sample size, shorter analysis time, and fewer manual operations, and it minimized processing contamination.

3.1.3. The UHPLC-HRMS method

For the chromatographic separation of target PFAS, three reversed-phase columns were evaluated: the Thermo Scientific Acclaim RSLC 120 C18 (2.1 × 100 mm, 2.2 μm), the Phenomenex Kinetex C18 (2.1 × 100 mm, 2.6 μm), and the Phenomenex Luna Omega PS C18 column (2.1 × 100 mm, 1.6 μm). Peak shape and retention time stability were assessed, with all columns performing well for the long-chain PFAS (C ≥ 8). However, the Luna Omega PS C18 column excelled for some short-chain congeners (PFBA, PFPeA, PFHxA, PFBS, and GenX) and telomers (4:2FTS, 6:2FTS, and 8:2FTS), offering improved retention and peak shapes (see Supplementary Information Fig. S4 and Fig. S5). The PS C18's mixed stationary phase comprises a C18 ligand and a positively charged surface and enables unique polar and non-polar interactions. This design enhances retention of acidic compounds through ionic/polar interactions. Consequently, the final method uses the PS C18 column, which is widely used in PFAS chromatographic separation [52,53]. .

Ensuring good chromatographic separation of target compounds is essential, but preventing contamination is equally vital for obtaining reliable results. As many components of HPLC systems contain per- and polyfluorinated compounds (PFCs), several measures were implemented to minimize PFAS background interference and contamination. Standard PFC-containing mobile-phase lines were replaced with PEEK tubing, a polypropylene cap insert, and stainless steel solvent inlet filters. To further reduce the background contamination, in particular from the mobile-phase, a Restek PFAS delay column (5 μm, 50 × 2.1 mm) was placed in the mobile phase flow path just before the injector. This delay column traps background PFAS before they reach the analytical column, while PFAS in the injected sample are focused onto the head of the analytical column and separated during the gradient analysis. Background PFAS retained in the delay column during equilibration are additionally retained, entering the analytical column only after the sample PFAS and emerging at the far-right end of the chromatogram. No background PFAS were detected from the mobile-phase components and HPLC tubing upstream the sample injection due to the ultra-high purity LC-MS grade solvents and PFC-free tubing and filter frits used. As a result, background contamination was never an issue. However, the performance of the delay column was evaluated by adding PFOA and PFOS standards (20 ng/L each) to the mobile phase. The results are provided in Fig. S9 of the Supplementary Information. The expected retention times of the "delayed" PFOA and PFOS were established, and the MS divert valve was programmed to direct the LC flow to the waste from 11 to 15 min and continued through the first 5 min (0–5 min) of the chromatographic run (details in Table 2), preventing any contaminants from entering the MS system.

According to ISO/IEC 17025:2017 [54], HRMS-based quantifications must confirm the molecular ion and at least one fragment ion, both with mass error less than 5 ppm. The critical MS and MS/MS parameters were optimized to achieve an optimal balance, enabling data collection in Full Scan and targeted MS/MS modes while meeting this requirement. The LC-HRMS data, including retention times, elemental composition, accurate mass, and monitored fragments, are provided in Table S2 (Supplementary Information). For C4–C8 perfluoalkylcarboxylic acids, the $[M\text{-}H]^-$ and $[M\text{-}CO_2\text{-}H]^-$ ions were monitored for the target and mass-labeled PFAS as the latter ion may be more abundant, particularly for PFBA and PFPeA [55]. Since analyte quantification in our method was based on isotope dilution, we compared the peak area ratios ($Area_{target}$ / $Area_{ILIS}$) of the $[M\text{-}H]^-$ and $[M\text{-}CO_2\text{-}H]^-$ pairs. The results indicated that the $[M\text{-}H]^-$ ions were the most abundant and also provided better repeatability (i.e., lower coefficients of variation). The data are reported in the Supplementary Information (Table S5). Target PFAS from PFCA and PFSA classes share the fragments with *m/z* 79.9561 and 98.9546, corresponding to $[SO_3]^{2-}$ and $[FSO_3]^-$, respectively. Another typical fragment for this class is *m/z* 118.9914, corresponding to $[C_2F_5]^-$. The long-chain PFCAs also have a common fragment with *m/z* 168.9885 ($[C_3F_7]^-$). Similarly, all the FTSs shared common fragments with *m/z* 80.9638 and *m/z* 79.9560. Quantification was not affected even for some of the analytes that eluted with close retention times since calculations were based on the unique high resolution accurate mass (HRAM) precursor ion ratios (analyte / internal standard). One of the advantages of high-resolution mass spectrometry is the ability to measure high-resolution accurate mass (HRAM) data in MS and MS/MS scans. As described in Section 2.6. *(Quality assurance and quality control)*, HRAM with mass error less than 2 ppm was maintained by calibrating the Orbitrap MS with the Pierce FlexMix calibration solution (external infusion), and by the introduction of the internal calibrant using the RunStart EASY-IC system before each sample injection. For most compounds, more than one qualifier ion was monitored. In the case of compounds eluting with close RT times (ΔRT ≤ 0.2 min), a unique fragment ion was selected among the multiple qualifier ions. For example, the ions with *m/z* 78 and 251 were used respectively FOSA and PFDoS (ΔRT = 0.2 min) in addition to the common ion *m/z* 99.

3.2. Method validation

Method validation and QA/QC procedures were carried out according to ISO/IEC 17025. Instrument performance was evaluated by injecting the QC sample (a mixture of mass-labeled standards) after 10 successive injections and determining instrument limits. The performance of the developed analytical method was evaluated by estimating linearity, LODs, LOQs, recovery, precision (inter-day and intraday repeatability), matrix effect, and carryover for each compound.

3.2.1. Matrix effect

Matrix effects (MEs) are a critical consideration in PFAS analysis due

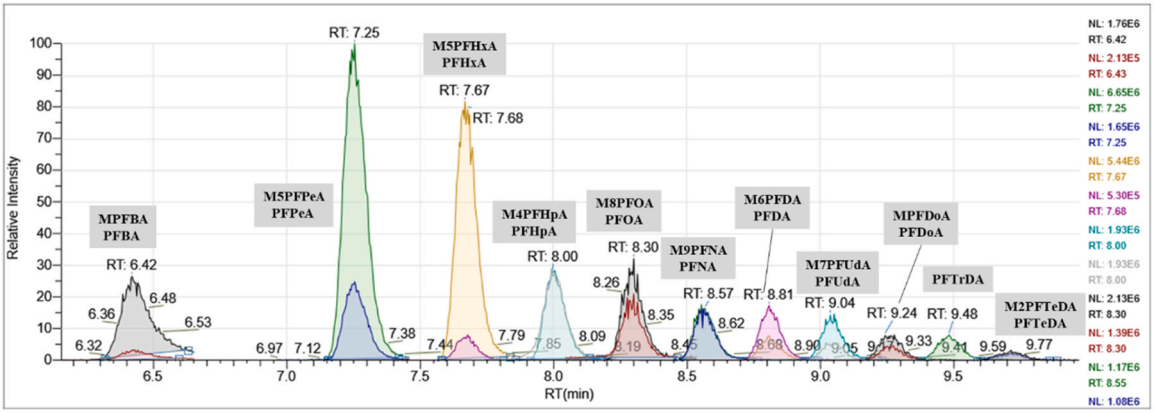

Fig. 5. : Chromatographic profiles of PFCA compounds and their internal standards. Shown are extracted ion chromatograms (XICs) of target compounds from the PFCA class and their corresponding ILISs. XICs for all target PFAS and ILISs are given in the Supplementary Information, Fig. S6.

to the complex nature of serum matrices, which can either suppress or enhance the analytical signal, potentially leading to inaccurate quantification. ME was evaluated statistically by comparing the slopes of an external calibration curve (Ext) and a standard addition curve (SAM), as described elsewhere [37,56]. The external calibration curve was constructed using nine standards (1.00, 5.00, 10.0, 20.0, 40.0, 60.0, 100, 250, and 500 ng/L) prepared in the injection diluent (20:80 methanol/water). The standard addition curve was constructed by spiking the newborn calf serum with 20.0, 40.0, and 60.0 ng/L of the target PFAS. In both cases, internal standards at constant concentration were added, and slopes were calculated using the peak area ratios (area of target PFAS to area of ILIS). The %ME was calculated as follows:

$$\%ME = \left[\left(\frac{Slope_{SAM}}{Slope_{Ext}}\right) * 100\right] - 100 \quad (1)$$

Following a *t*-test, the comparison of the slopes can give a %ME = 0 (no matrix effect), %ME< 0 (signal suppression), or %ME> 0 (signal enhancement). Serum concentrations of PFOS, PFOA, and PFHxS may vary between the ng/L and μg/mL ranges. In the latter situation, substantial dilution of serum samples is required to adjust PFAS concentrations to within the method's linear range. In the current work, the matrix effect was evaluated for 1:10 and 1:100 (v/v) diluted serum samples. The results show that a matrix effect was present for all compounds in the 1:10 diluted samples (Fig. S7, Supplementary Information); consequently, quantification was performed using the SAM approach. The matrix effect was not present for serum samples diluted 1:100, allowing for quantification using six-point calibration curves in the range of 1–500 ng/L prepared from native PFAS standards in water/methanol (80:20, v/v).

3.2.2. Linearity, LOD, and LOQ

Linearity was evaluated by constructing calibration curves, calculating the coefficient of determination (R^2), and performing the lack-of-fit (LOF) test. Calibration curves were obtained by plotting the peak area ratio of each target PFAS to the corresponding ILIS (y-axis) against concentration (x-axis). The method's LODs and LOQs were determined using the ISO-accepted Hubaux-Vos methodology [38]. This method simplifies the determination of method variability at the blank level (σ_b) when the instrument response is linearly proportional to concentration and all calibration standards have a constant error distribution (are homoscedastic). To calculate σ_b from a linear calibration curve, either the regression residual standard deviation (s_{res}) or the y-intercept standard deviation (s_{b0}) can be used. The results are summarized in Table 3. All the calibration curves were linear in the concentration ranges studied ($R^2 > 0.977$), with no lack-of-fit. LODs and LOQs ranged from 4.3 to 13 ng/L and from 8.9 to 27 ng/L, respectively, confirming the high sensitivity of this method. LODs and LOQs reported in Table 3 were calculated with both the Hubaux-Vos method and the ICH method [39]. According to the ICH method, LOD and LOQ values are based on the calibration curve's standard deviation of residuals, $s_{(y/x)}$:

$$LOD = 3{\cdot}3 * s_{(y/x)}/Slope \quad (2)$$

$$LOQ = 10 * s_{(y/x)}/Slope \quad (3)$$

LODs calculated by the two approaches are very similar, but LOQs calculated by the ICH approach appear higher. The values calculated by the Hubaux-Vos method were retained as the most reliable since they properly exploit the uncertainty of the calibration curve. In the case of PFOS and PFOA, the matrix already contained a quantity of analyte greater than the calculated LOD. This may affect the LOD and LOQ estimations using the standard Hubaux-Vos method. For these two analytes, it was necessary to estimate the LOD and LOQ values for a matrix free of these two molecules. To this end, in the case of the Hubaux-Vos method, we proceeded as follows. First, the mean blank signal (for PFOS and PFOA) was subtracted from the standard addition curve. Next, the procedure provided by the Hubaux-Vos method was applied to the new curve, but the signal related to the point where the upper confidence band meets the y-axis (for the calculation of the critical limit) was increased by a value equal to the error associated with the mean blank subtraction. This was done in order to take into account the signal subtracted from the calibration curve. Indeed, the correction

Table 3
Method validation parameters: calibration range, linearity (R^2), LOD and LOQ.

Compounds	Range (ng/L)	Hubaux-Vos method		ICH method		R^2
		LOD (ng/L)	LOQ (ng/L)	LOD (ng/L)	LOQ (ng/L)	
PFBA	0.00 - 60.0	6.9	14	8.5	26	0.989
PFPeA	0.00 - 60.0	6.9	14	6.8	21	0.993
PFHxA	0.00 - 60.0	5.0	8.9	5.0	15	0.996
PFHpA	0.00 - 60.0	5.5	12	5.4	17	0.996
PFOA	0.00 - 60.0	8.8	13	7.6	23	0.991
PFNA	0.00 - 60.0	8.5	18	8.4	25	0.989
PFDA	0.00 - 60.0	5.3	10	5.3	16	0.996
PFUdA	0.00 - 60.0	7.3	17	7.6	23	0.991
PFDoA	0.00 - 60.0	7.7	17	7.3	22	0.991
PFTrDA	0.00 - 60.0	9.6	21	9.0	27	0.987
PFTeDA	0.00 - 60.0	7.1	16	6.7	20	0.993
PFBS	0.00 - 60.0	6.6	14	6.5	20	0.994
PFPeS	0.00 - 60.0	6.8	14	6.6	20	0.993
PFHxS	0.00 - 60.0	5.6	12	5.5	17	0.995
PFHpS	0.00 - 60.0	10	24	10	31	0.983
PFOS	0.00 - 60.0	9.3	13	7.9	24	0.991
PFNS	0.00 - 60.0	8.3	17	8.1	25	0.990
PFDS	0.00 - 60.0	11	24	11	35	0.980
PFDoS	0.00 - 60.0	11	27	10	33	0.983
HFPO-DA	0.00 - 60.0	5.2	13	5.3	16	0.996
ADONA	0.00 - 60.0	5.6	12	5.4	16	0.995
FOSA	0.00 - 60.0	4.3	9.1	4.2	13	0.997
MeFOSA	0.00 - 60.0	8.7	18	8.5	26	0.989
EtFOSA	0.00 - 60.0	11	25	11	33	0.981
FOSAA	0.00 - 60.0	13	27	11	36	0.977
MeFOSAA	0.00 - 60.0	9.3	13	9.1	28	0.988
EtFOSAA	0.00 - 60.0	8.0	17	7.6	23	0.991
4:2FTS	0.00 - 60.0	5.1	11	5.1	15	0.996
6:2FTS	0.00 - 60.0	7.0	12	6.9	21	0.993
8:2FTS	0.00 - 60.0	9.4	21	8.8	27	0.987
PFEESA	0.00 - 60.0	7.3	15	7.2	22	0.992
Nafion-BP2	0.00 - 60.0	5.3	11	5.3	16	0.996

corresponds to the standard deviation of the subtraction. The error thus increased is therefore propagated in the calculation of the critical limit, the LOD, and the LOQ.

The LODs for most analytes included in the current method were less than 10 ng/L, making it 5 to 15 times more sensitive than previously reported methods (see Table S3 in the Supplementary Information for detailed comparison data).

3.2.3. Precision and accuracy

The intraday and interday precision and accuracy of the method were estimated by analyzing five replicates of serum spiked at two different QC levels, 10.0 and 50.0 ng/L. Precision was estimated by calculating the relative standard deviation (RSD) of the results of the analysis of QC samples in five replicates on the same day (n = 5, intraday precision) and the analysis of five replicates of the QC samples on three consecutive days ($n = 15$, interday precision). The method accuracy was calculated on the basis of PFAS recoveries, which were evaluated by spiking the serum samples at two QC levels (QC_1 = 10.0 ng/L and QC_2 = 50.0 ng/L). Spiked and unspiked serum samples were prepared in triplicate, and the PFAS concentrations in the unspiked (C_{us}) and spiked (C_{ss}) serums were determined. Percentage recoveries (% R) were calculated in relation to the actual concentration of spiked PFAS (C_s).

$$Recovery(\%R) = \left(\frac{C_{SS} - C_{US}}{C_S}\right) * 100 \quad (4)$$

Recoveries ranged from 72.7 to 97.8 % for QC_1 and 72.9 to 106 % for QC_2. High precision and recovery rates across both QC levels underline the method's reproducibility and reliability in quantifying PFAS even at the low concentrations often found in serum samples.

3.2.4. Carryover effect

Stringent control of carryover is essential to maintain the accuracy and reliability of the method during high-throughput analyses and to ensure that each sample's results are independent of previous injections. Carryover was also carefully evaluated by injecting three blanks after the highest concentration standard of the calibration curve. A criterion was set in the quantification method, requiring less than 0.05 % carryover in the blank sample. The autosampler loop and needle were washed for about 4.5 min with a mixture of acetonitrile and methanol (50:50, v/v), represented as C in Table 1; thus, no carryover was detected for any of the target analytes.

3.3. Control charts

Shewhart's and CUSUM control charts were employed to monitor the method's performance over time, ensuring consistent results and identifying the need for maintenance, particularly when analyzing large batches of samples. This method was developed with the purpose of routinely analyzing many samples. When analyzing many samples over a period of several days, the ideal mass spectrometer must be able to withstand small variations in uncontrollable factors to ensure accurate measurements. The atmospheric pressure ionization source and ion transfer tubes become contaminated over time. If not properly cleaned, they can have detrimental effects on the sensitivity, mass accuracy, and intensity of precursor and fragment ions. The frequency with which the mass spectrometer's components must be cleaned is determined by the types and amounts of samples and solvents used in the instrument. If a decline in performance is identified, the MS components can be cleaned to restore the desired performance. In this context, we performed experiments to evaluate the mass spectrometer's stability over time.

The LC–MS performance was monitored by running the standard addition curve (0.0, 20.0, 40.0, and 60.0 ng/L) at the beginning of the batch and after every 10 samples (serum spiked at 30 ng/L of the 32 PFAS). The Thermo Scientific EASY-IC source uses an internal calibrant, which guarantees a consistently high mass accuracy (< 2 ppm error) over 5 days. During sample analysis, the mass was calibrated before each sample injection using the internal calibrant RunStart EASY-IC system. Additionally, the Orbitrap MS was calibrated externally with the Pierce FlexMix calibration solution on the first day of analysis. The LC–MS system operated nonstop for 3 days, analyzing a total of 240 samples (standard addition curve, samples, and blanks).

The consistency of the standard addition curve was evaluated using Shewhart's control charts. The mean (average) and range charts were used to monitor the slope of the standard addition curve. The range charts are not reported here since no deviation from the "in-control" situation was recorded. Regarding the mean charts, the average slope value of the SAM calibration curve for each analyte (M) was used as a reference, with upper and lower control limits set to ± 20 % matrix effect (M ± 20 %). Classical ± 3σ Shewhart's control limits were also calculated but are not reported in the graphics since they were very wide. Furthermore, the reliability of the quantitative data calculated for the samples was evaluated using peak area ratios (target peak to ILIS peak).

Regarding control charts, the analytes could be divided into four main groups with slightly different behaviors: importantly, all the control charts followed trends roughly comparable to one of these four groups. Fig. 6 shows four examples of Shewhart's and CUSUM charts, one for each group (G1–G4). The control charts report the samples on the x-axis in temporal order, while the slope (Shewhart's charts) or the cumulative sums (CUSUM charts) are reported on the y-axes. The G1 group shows quite stable behavior for the first 2 days (first 14 measurements on the x-axis), then the slope decreases and shows values below the average, as can also be noticed in the CUSUM chart, showing a negative trend particularly evident after around 14 measurements. The analytes that behave in this way are PFBA, PFPeA, 4:2FTS, PFBS, PFHpA, PFHxS, 6:2FTS, PFOS, PFUdA, PFDoA, and PFDA. The Shewhart's chart for the group G2 is similar to that for G1 but, in this case, the CUSUM chart records first a slight decrease in the slope, then the CUSUM reaches a sort of stability, and then another negative trend is evident: this is the behavior of PFHxA and PFPeS. No out-of-control condition was detected, as the slopes for all target analytes were within the control limits, demonstrating the high level of stability of the standard addition curve. The largest group was G3, displaying a gradual decrease in slope, although this trend is less apparent during the initial 2 days (up to number 14) and becomes more noticeable on day 3. This behavior is characteristic of PFEESA, HFPO-DA, ADONA, Nafion byproduct 2, PFOA, PFHpS, PFNA, MeFOSA, EtFOSA, FOSA, PFTrDA, and PFTeDA. The last group, G4, shows more stable behavior for the first 2 days and then a sudden decrease in the slope; it comprises PFNS, EtFOSAA, PFDoS, 8:2FTS, and MeFOSAA.

According to the CUSUM results, it seems that there is a trend in the first 14 measurements. However, it is worth noting that CUSUM, unlike the Shewhart chart, is sensitive to small shifts by accumulating deviations over time [57]. After careful analysis of the results, the shifts observed in the first 14 measurements were found to be not significant because they were below the LODs and LOQs for all compounds. Therefore, neither compound detection nor quantification were affected. Moreover, since the shifts highlighted by the CUSUM charts within the first 14 measurements are very low (e.g., 3.0×10^{-3} in G4), a shift of concentration greater than the LODs would not be possible in this time frame. Since in all cases the most relevant deviations occurred during the third day of analysis, the final standard operating procedure (SOP) states the necessity of cleaning the mass spectrometer's ionization source every 2 days of routine analysis.

3.4. UHPLC-HRMS analysis of real samples

To evaluate the suitability of the validated method, blood samples obtained from five individuals, who are all co-authors of this article, were subjected to analysis using the complete method as described. .

Fig. 6. : Shewhart (left) and CUSUM (right) control charts. The graphs depict the samples on the *x*-axis in chronological sequence, while the *y*-axes present the slope (in Shewhart's charts) or the cumulative sums (in CUSUM charts). The analytes were classified into four categories based on the trends observed for the Shewhart (a–d) and corresponding CUSUM (e–h) control charts.

Table 5 provides details on the quantification and detection frequency of compounds detected at concentrations equal to or greater than the limit of quantification (≥LOQ) in at least one sample. The complete table, which includes the results for all compounds with concentrations below the LOQ, can be found in Table S4 (Supplementary Information). Results are presented as the median and 5th and 95th percentiles, and the number of samples with concentrations ≥LOQ and the corresponding percentage. For the purpose of calculating the median and percentiles, non-quantifiable values were substituted with half of the LOQ. The highest median levels were obtained for PFOS (2.400 μg/L) and PFOA (1.118 μg/L). We achieved a 100 % detection rate for some PFCAs (PFHxA, PFHpA, PFOA, PFNA, and PFDA) and PFSAs (PFHxS, PFHpS, and PFOS). The short-chain homologues (PFBA, PFPeA, PFBS, and PFPeS) and other emerging PFAS including GenX, ADONA, PFEESA,

Table 4
Precision (intraday and interday) and recovery data for serum samples spiked with QC_1 (10.0 ng/L) and QC_2 (50.0 ng/L) of the target PFAS. Spike concentrations were within the standard addition curves used for quantification (0.0–60.0 ng/L).

Compounds	Intraday RSD		Interday RSD		%Recovery (± RSD)	
	QC_1	QC_2	QC_1	QC_2	QC_1	QC_2
PFBA	3.4	11	4.9	4.6	97.4 (9.8)	106 (5.6)
PFPeA	4.9	5.2	4.0	3.3	93.6 (3.7)	90.3 (4.3)
PFHxA	4.4	9.1	3.4	6.0	89.9 (6.5)	93.2 (5.9)
PFHpA	4.7	7.9	2.9	3.9	93.1 (4.1)	95.3 (4.5)
PFOA	4.6	7.6	2.3	6.7	87.1 (1.8)	91.0 (3.0)
PFNA	4.4	5.0	2.1	3.5	82.8 (2.1)	88.7 (2.1)
PFDA	4.6	7.1	2.1	5.4	91.2 (3.3)	93.4 (1.4)
PFUdA	3.9	7.3	3.7	6.6	92.1 (5.5)	95.0 (4.2)
PFDoA	4.6	9.2	4.5	7.4	97.8 (7.2)	103 (6.0)
PFTrDA	6.2	9.9	3.6	7.5	91.0 (8.6)	88.5 (2.2)
PFTeDA	4.1	3.4	2.4	6.8	85.5 (2.3)	84.7 (3.0)
PFBS	5.5	6.3	3.4	7.9	85.6 (4.4)	84.5 (4.3)
PFPeS	4.8	4.0	2.4	4.6	91.8 (6.2)	83.6 (1.6)
PFHxS	5.6	9.7	2.3	4.3	91.7 (3.9)	90.4 (1.4)
PFHpS*	3.0	2.7	1.9	4.4	86.3 (3.8)	92.4 (6.3)
PFOS	3.6	4.7	2.1	5.1	93.2 (5.6)	90.6 (1.6)
PFNS	4.1	4.5	3.9	4.8	76.2 (8.2)	76.9 (3.5)
PFDS*	6.5	7.0	5.1	5.0	96.3 (1.7)	96.2 (4.1)
PFDoS*	5.8	6.2	3.6	7.8	76.8 (5.8)	75.4 (5.9)
FOSA	3.5	4.4	6.1	5.1	93.1 (3.9)	93.5 (4.2)
MeFOSA	4.4	4.3	1.5	7.9	87.7 (5.0)	90.7 (3.1)
MeFOSAA	2.6	5.7	1.3	6.2	93.0 (2.7)	93.4 (2.2)
FOSAA*	5.2	14	4.5	9.2	79.0 (3.5)	80.7 (3.4)
EtFOSA*	6.3	10	4.9	11	74.1 (1.9)	72.9 (1.7)
EtFOSAA	9.0	4.6	5.7	5.9	80.4 (3.9)	85.8 (5.2)
HFPO-DA	8.7	7.2	9.6	7.3	72.7 (2.7)	75.7 (2.9)
ADONA	5.7	9.1	3.0	4.2	80.8 (8.5)	84.6 (5.3)
4:2FTS	7.3	7.5	3.6	4.7	91.5 (4.9)	84.2 (2.2)
6:2FTS	4.5	4.6	2.1	6.0	97.4 (8.0)	93.4 (3.7)
8:2FTS	2.7	5.0	3.7	6.0	93.0 (3.1)	92.4 (4.0)
PFEESA	3.9	6.5	1.6	2.2	74.5 (2.7)	80.3 (1.3)
Nafion BP2	2.9	6.1	2.4	5.3	93.9 (3.3)	94.8 (7.2)

* QC_1 was 15 ng/L since the LODs of these analytes were slightly higher than 10 ng/L.

Table 5
Results of human serum analysis: application of the method to five human serum samples.

Compound	5^{th} percentile (μg/L)	Median (μg/L)	95^{th} percentile (μg/L)	# Samples ≥ LOQ (percentage)
PFHxA	0.017	0.019	0.057	5 (100 %)
PFHxS	0.081	0.248	0.530	5 (100 %)
PFHpA	0.013	0.019	0.039	5 (100 %)
PFHpS	0.016	0.035	0.130	5 (100 %)
PFOA	0.545	0.855	1.118	5 (100 %)
PFOS	0.741	1.120	2.400	5 (100 %)
PFNA	0.090	0.156	0.392	5 (100 %)
PFDA	0.048	0.092	0.386	5 (100 %)
PFUdA	<LOQ	0.0410	0.295	4 (80 %)
PFDoA	<LOQ	<LOQ	0.023	1 (20 %)

and Nafion BP-2 were not found in any of the samples.

4. Future perspectives and conclusions

A new, highly sensitive method has been developed and validated to accurately quantify 32 PFAS in human serum using online SPE-UHPLC-HRMS. The sample pretreatment developed in this study can greatly enhance the accuracy of PFAS determination in human serum. Our results demonstrate that much improved PFAS recoveries can be achieved by combining PP with pellet rinsing followed by online SPE pretreatment. WAX online SPE sorbent is preferred especially for short chain PFAS congeners (C4–C6). Furthermore, compared with traditional reversed–phase C18 columns, the additional positively charged surface in the Luna Omega PS C18 column favored the retention of short chain PFCA, PFSA, and FTS compounds.

The current method achieved very low limits of detection (LODs <10 ng/L for 27 analytes), which are 5 to 15 times lower than those in previous studies. Various considerations and optimizations contributed to this improvement. They include the use of certified PFC-free polypropylene vials, installing a delay column to trap possible PFAS contamination from the HPLC system, optimizing the sample pretreatment (PP and SPE), and selecting a suitable column for chromatographic separation. The online SPE-UHPLC-HRMS analysis time was relatively fast, requiring only 16 min per injection. The detection of PFOA and PFOS in the newborn calf serum forced us to apply special measures, which led to a lengthy method validation process. It is worth mentioning that commercial availability of certified PFAS-free human serum or another matrix-matched serum such as fetal bovine serum would greatly benefit the development of new methods for PFAS analysis.

The validated method was successfully used to analyze serum samples obtained from five individuals with no history of direct PFAS exposure. Ten PFAS were detected, of which eight were found in all five individuals. The highest median recorded concentration was for PFOS (1.12 μg/mL). This simple and reliable method allows for high-throughput PFAS profiling from serum and is well-suited for biological monitoring of both legacy and emerging PFAS in humans. This method can be used for routine human serum sample analysis; however, it requires regular cleaning of the mass spectrometer's ionization source after every 2 days of continuous operation. Finally, we emphasize the significance of establishing regular interlaboratory calibration/comparison studies. With the participation of a network of laboratories with excellent analytical comparability and accuracy, new methods, including the one described here, may be intercalibrated/compared with others to supplement the standard in-house validation.

CRediT authorship contribution statement

Masho Hilawie Belay: Writing – review & editing, Writing – original draft, Visualization, Validation, Supervision, Software, Methodology, Investigation, Formal analysis, Data curation, Conceptualization. **Elisa Robotti**: Writing – review & editing, Writing – original draft, Visualization, Validation, Supervision, Software, Resources, Methodology, Investigation, Data curation, Conceptualization. **Arianna Ghignone**: Writing – review & editing, Writing – original draft, Validation, Software, Formal analysis, Data curation. **Alessia Fabbris**: Writing – review & editing, Writing – original draft, Validation, Software, Formal analysis, Data curation. **Jessica Brandi**: Validation, Methodology, Investigation, Data curation. **Daniela Cecconi**: Validation, Methodology, Investigation, Data curation. **Maria Angela Masini**: Writing – review & editing. **Francesco Dondero**: Resources, Project administration, Funding acquisition. **Emilio Marengo**: Writing – review & editing, Supervision, Methodology, Conceptualization.

Environmental implication

PFAS constitute a broad class of environmental contaminants known for their endocrine-disrupting properties and persistence in the environment, which leads to their accumulation in the human body and subsequent hazardous effects on human health. The method presented here for the determination of 32 PFAS, including both legacy and emerging compounds, in human serum has been meticulously optimized to ensure reliable, sensitive, and accurate measurements. The incorporation of online solid-phase extraction (SPE) enhances sample cleanup and concentration, improving the method's overall efficiency and sensitivity. This method establishes a robust foundation for future biomonitoring and assessment of human exposure to PFAS.

Declaration of Competing Interest

The authors declare that they have no known competing financial interests or personal relationships that could have appeared to influence the work reported in this paper.

Acknowledgements

This project has received funding from the European Union's Horizon 2020 research and innovation program under grant agreement No 101037509 (SCENARIOS project).

Appendix A. Supporting information

Supplementary data associated with this article can be found in the online version at doi:10.1016/j.jhazmat.2024.136780.

Data availability

Data will be made available on request.

References

[1] Brase, R.A., Mullin, E.J., Spink, D.C., 2021. Legacy and emerging per-and polyfluoroalkyl substances: analytical techniques, environmental fate, and health effects. Int J Mol Sci 22, 995. https://doi.org/10.3390/ijms22030995.

[2] The Interstate Technology & Regulatory Council (ITRC), 2024. Technical resources for addressing environmental releases of per- and polyfluoroalkyl substances (PFAS). ⟨https://pfas-1.itrcweb.org/⟩ (accessed 9 August 2024).

[3] Gaines, L.G., 2023. Historical and current usage of per-and polyfluoroalkyl substances (PFAS): a literature review. Am J Ind Med 66, 353–378. https://doi.org/10.1002/ajim.23362.

[4] Kurwadkar, S., Dane, J., Kanel, S.R., Nadagouda, M.N., Cawdrey, R.W., Ambade, B., Struckhoff, G.C., Wilkin, R., 2022. Per-and polyfluoroalkyl substances in water and wastewater: a critical review of their global occurrence and distribution. Sci Total Environ 809, 151003. https://doi.org/10.1016/j.scitotenv.2021.151003.

[5] Androulakakis, A., Alygizakis, N., Bizani, E., Thomaidis, N.S., 2022. Current progress in the environmental analysis of poly-and perfluoroalkyl substances (PFAS). Environ Sci: Adv 1, 705–724. https://doi.org/10.1039/d2va00147k.

[6] Junttila, V., Vähä, E., Perkola, N., Räike, A., Siimes, K., Mehtonen, J., Kankaanpää, H., Mannio, J., 2019. PFASs in Finnish rivers and fish and the loading of PFASs to the Baltic Sea. Water 11, 870. https://doi.org/10.3390/w11040870.

[7] Ateia, M., Maroli, A., Tharayil, N., Karanfil, T., 2019. The overlooked short-and ultrashort-chain poly-and perfluorinated substances: a review. Chemosphere 220, 866–882. https://doi.org/10.1016/j.chemosphere.2018.12.186.

[8] Zhong, M., Wang, T., Qi, C., Peng, G., Lu, M., Huang, J., Blaney, L., Yu, G., 2019. Automated online solid-phase extraction liquid chromatography tandem mass spectrometry investigation for simultaneous quantification of per-and polyfluoroalkyl substances, pharmaceuticals and personal care products, and organophosphorus flame retardants in environmental waters. J Chromatogr A 1602, 350–358. https://doi.org/10.1016/j.chroma.2019.06.012.

[9] Lind, P.M., Lind, L., Salihovic, S., Ahlström, H., Michaelsson, K., Kullberg, J., Strand, R., 2022. Serum levels of perfluoroalkyl substances (PFAS) and body composition–A cross-sectional study in a middle-aged population. Environ Res 209, 112677. https://doi.org/10.1016/j.envres.2022.112677.

[10] Frigerio, G., Cafagna, S., Polledri, E., Mercadante, R., Fustinoni, S., 2022. Development and validation of an LC–MS/MS method for the quantitation of 30 legacy and emerging per-and polyfluoroalkyl substances (PFASs) in human plasma, including HFPO-DA, DONA, and cC6O4. Anal Bioanal Chem 414, 1259–1278. https://doi.org/10.1007/s00216-021-03762-1.

[11] Beser, M.I., Pardo, O., Beltrán, J., Yusà, V., 2019. Determination of 21 perfluoroalkyl substances and organophosphorus compounds in breast milk by liquid chromatography coupled to orbitrap high-resolution mass spectrometry. Anal Chim Acta 1049, 123–132. https://doi.org/10.1016/j.aca.2018.10.033.

[12] Kourtchev, I., Hellebust, S., Heffernan, E., Wenger, J., Towers, S., Diapouli, E., Eleftheriadis, K., 2022. A new on-line SPE LC-HRMS method for the analysis of Perfluoroalkyl and Polyfluoroalkyl Substances (PFAS) in PM2. 5 and its application for screening atmospheric particulates from Dublin and Enniscorthy, Ireland. Sci Total Environ 835, 155496. https://doi.org/10.1016/j.scitotenv.2022.155496.

[13] Khan, B., Burgess, R.M., Cantwell, M.G., 2023. Occurrence and bioaccumulation patterns of per-and polyfluoroalkyl substances (PFAS) in the marine environment. ACS EST Water 3, 1243–1259. https://doi.org/10.1021/acsestwater.2c00296.

[14] Death, C., Bell, C., Champness, D., Milne, C., Reichman, S., Hagen, T., 2021. Per-and polyfluoroalkyl substances (PFAS) in livestock and game species: A review. Sci Total Environ 774, 144795. https://doi.org/10.1016/j.scitotenv.2020.144795.

[15] Espartero, L.J.L., Yamada, M., Ford, J., Owens, G., Prow, T., Juhasz, A., 2022. Health-related toxicity of emerging per-and polyfluoroalkyl substances: Comparison to legacy PFOS and PFOA. Environ Res 212, 113431. https://doi.org/10.1016/j.envres.2022.113431.

[16] Xu, B., Liu, S., Zhou, J.L., Zheng, C., Weifeng, J., Chen, B., Zhang, T., Qiu, W., 2021. PFAS and their substitutes in groundwater: occurrence, transformation and remediation. J Hazard Mater 412, 125159. https://doi.org/10.1016/j.jhazmat.2021.125159.

[17] Nian, M., Zhou, W., Feng, Y., Wang, Y., Chen, Q., Zhang, J., 2022. Emerging and legacy PFAS and cytokine homeostasis in women of childbearing age. Sci Rep 12, 6517. https://doi.org/10.1038/s41598-022-10501-8.

[18] Yang, L.H., Yang, W.J., Lv, S.H., Zhu, T.T., Sharif, H.M.A., Yang, C., Du, J., Lin, H., 2022. Is HFPO-DA (GenX) a suitable substitute for PFOA? A comprehensive degradation comparison of PFOA and GenX via electrooxidation. Environ Res 204, 111995. https://doi.org/10.1016/j.envres.2021.111995.

[19] Yao, W., Xu, J., Tang, W., Gao, C., Tao, L., Yu, J., Lv, J., Wang, H., Fan, Y., Xu, D.X., Huang, Y., 2023. Developmental toxicity of perfluorohexane sulfonate at human relevant dose during pregnancy via disruption in placental lipid homeostasis. Environ Int 177, 108014. https://doi.org/10.1016/j.envint.2023.108014.

[20] De Silva, A.O., Armitage, J.M., Bruton, T.A., Dassuncao, C., Heiger-Bernays, W., Hu, X.C., Kärrman, A., Kelly, B., Ng, C., Robuck, A., Sun, M., 2021. PFAS exposure pathways for humans and wildlife: a synthesis of current knowledge and key gaps in understanding. Environ Toxicol Chem 40, 631–657. https://doi.org/10.1002/etc.4935.

[21] Zhuchen, H.Y., Wang, J.Y., Liu, X.S., Shi, Y.W., 2023. Research progress on neurodevelopmental toxicity in offspring after indirect exposure to PFASs in early life. Toxics 11, 571. https://doi.org/10.3390/toxics11070571.

[22] Sunderland, E.M., Hu, X.C., Dassuncao, C., Tokranov, A.K., Wagner, C.C., Allen, J. G., 2019. A review of the pathways of human exposure to poly-and perfluoroalkyl substances (PFASs) and present understanding of health effects. J Expo Sci Environ Epidemiol 29, 131–147. https://doi.org/10.1038/s41370-018-0094-1.

[23] Bonato, M., Corrà, F., Bellio, M., Guidolin, L., Tallandini, L., Irato, P., Santovito, G., 2020. PFAS environmental pollution and antioxidant responses: an overview of the impact on human field. Int J Environ Res Public Health 17, 8020. https://doi.org/10.3390/ijerph17218020.

[24] Gao, K., Fu, J., Xue, Q., Li, Y., Liang, Y., Pan, Y., Zhang, A., Jiang, G., 2018. An integrated method for simultaneously determining 10 classes of per-and polyfluoroalkyl substances in one drop of human serum. Anal Chim Acta 999, 76–86. https://doi.org/10.1016/j.aca.2017.10.038.

[25] Richterová, D., Govarts, E., Fábelová, L., Rausová, K., Martin, L.R., Gilles, L., Remy, S., Colles, A., Rambaud, L., Riou, M., Gabriel, C., 2023. PFAS levels and determinants of variability in exposure in European teenagers–Results from the HBM4EU aligned studies (2014–2021). Int J Hyg Envir Health 247, 114057. https://doi.org/10.1016/j.ijheh.2022.114057.

[26] Pitter, G., Da Re, F., Canova, C., Barbieri, G., Zare Jeddi, M., Daprà, F., Manea, F., Zolin, R., Bettega, A.M., Stopazzolo, G., Vittorii, S., 2020. Serum levels of perfluoroalkyl substances (PFAS) in adolescents and young adults exposed to contaminated drinking water in the Veneto region, Italy: a cross-sectional study based on a health surveillance program. Environ Health Perspect 128, 027007. https://doi.org/10.1289/EHP5337.

[27] Kuo, K.Y., Chen, Y., Chuang, Y., Lin, P., Lin, Y.J., 2023. Worldwide serum concentration-based probabilistic mixture risk assessment of perfluoroalkyl substances among pregnant women, infants, and children. Ecotoxicol Environ Saf 268, 115712. https://doi.org/10.1016/j.ecoenv.2023.115712.

[28] Sonnenberg, N.K., Ojewole, A.E., Ojewole, C.O., Lucky, O.P., Kusi, J., 2023. Trends in serum per-and polyfluoroalkyl substance (PFAS) concentrations in teenagers and adults, 1999–2018 NHANES. Int J Environ Res Public Health 20, 6984. https://doi.org/10.3390/ijerph20216984.

[29] Belay, M.H., Precht, U., Mortensen, P., Marengo, E., Robotti, E., 2022. A fully automated online SPE-LC-MS/MS method for the determination of 10 pharmaceuticals in wastewater samples. Toxics 10, 103. https://doi.org/10.3390/toxics10030103.

[30] Jimenez-Skrzypek, G., González-Sálamo, J., Hernandez-Borges, J., 2023. Analytical methodologies and occurrence of per-and polyfluorinated alkyl substances–A review. J Chromatogr Open, 100089. https://doi.org/10.1016/j.jcoa.2023.100089.

[31] Nakayama, S.F., Isobe, T., Iwai-Shimada, M., Kobayashi, Y., Nishihama, Y., Taniguchi, Y., Sekiyama, M., Michikawa, T., Yamazaki, S., Nitta, H., Oda, M., 2020. Poly-and perfluoroalkyl substances in maternal serum: method development and application in Pilot Study of the Japan Environment and Children's Study. J Chromatogr A 1618, 460933. https://doi.org/10.1016/j.chroma.2020.460933.

[32] Kato, K., Kalathil, A.A., Patel, A.M., Ye, X., Calafat, A.M., 2018. Per-and polyfluoroalkyl substances and fluorinated alternatives in urine and serum by on-line solid phase extraction–liquid chromatography–tandem mass spectrometry. Chemosphere 209, 338–345. https://doi.org/10.1016/j.chemosphere.2018.06.085.

[33] Poothong, S., Lundanes, E., Thomsen, C., Haug, L.S., 2017. High throughput online solid phase extraction-ultra high performance liquid chromatography-tandem mass spectrometry method for polyfluoroalkyl phosphate esters, perfluoroalkyl phosphonates, and other perfluoroalkyl substances in human serum, plasma, and whole blood. Anal Chim Acta 957, 10–19. https://doi.org/10.1016/j.aca.2016.12.043.

[34] Liu, Y., D'Agostino, L.A., Qu, G., Jiang, G., Martin, J.W., 2019. High-resolution mass spectrometry (HRMS) methods for nontarget discovery and characterization of poly-and per-fluoroalkyl substances (PFASs) in environmental and human samples. TrAC 121, 115420. https://doi.org/10.1016/j.trac.2019.02.021.

[35] Nakayama, S.F., Yoshikane, M., Onoda, Y., Nishihama, Y., Iwai-Shimada, M., Takagi, M., Kobayashi, Y., Isobe, T., 2019. Worldwide trends in tracing poly-and

perfluoroalkyl substances (PFAS) in the environment. TrAC 121, 115410. https://doi.org/10.1016/j.trac.2019.02.011.
[36] Al Amin, M., Sobhani, Z., Liu, Y., Dharmaraja, R., Chadalavada, S., Naidu, R., Chalker, J.M., Fang, C., 2020. Recent advances in the analysis of per-and polyfluoroalkyl substances (PFAS)—A review. Environ Technol Innov 19, 100879. https://doi.org/10.1016/j.eti.2020.100879.
[37] Ito, S., Tsukada, K., 2002. Matrix effect and correction by standard addition in quantitative liquid chromatographic–mass spectrometric analysis of diarrhetic shellfish poisoning toxins. J Chromatogr A 943, 39–46. https://doi.org/10.1016/S0021-9673(01)01429-7.
[38] Hubaux, A.V., Decision, G., 1970. detection limits for linear calibration curves. Anal Chem 42, 849–855. https://doi.org/10.1021/ac60290a013.
[39] International Conference on Harmonization (ICH) harmonized tripartite guideline, 2005. Validation of analytical procedures: text and methodology. Q2 (R1), 1(20), p.05.
[40] Shewhart, W.A., 1938. Application of statistical methods to manufacturing problems. J Frank Inst 226, 163–186. https://doi.org/10.1016/S0016-0032(38)90436-3.
[41] Chang, T.C., Gan, F.F., 1995. A cumulative sum control chart for monitoring process variance. J Qual Technol 27, 109–119. https://doi.org/10.1080/00224065.1995.11979574.
[42] Gosetti, F., Belay, M.H., Marengo, E., Robotti, E., 2020. Development and validation of a UHPLC-MS/MS method for the identification of irinotecan photodegradation products in water samples. Environ Pollut 256, 113370. https://doi.org/10.1016/j.envpol.2019.113370.
[43] Bangma, J., McCord, J., Giffard, N., Buckman, K., Petali, J., Chen, C., Amparo, D., Turpin, B., Morrison, G., Strynar, M., 2023. Analytical method interferences for perfluoropentanoic acid (PFPeA) and perfluorobutanoic acid (PFBA) in biological and environmental samples. Chemosphere 315, 137722. https://doi.org/10.1016/j.chemosphere.2022.137722.
[44] Da Silva, B.F., Ahmadireskety, A., Aristizabal-Henao, J.J., Bowden, J.A., 2020. A rapid and simple method to quantify per-and polyfluoroalkyl substances (PFAS) in plasma and serum using 96-well plates. MethodsX 7, 101111. https://doi.org/10.1016/j.mex.2020.101111.
[45] Starnes, H.M., Jackson, T.W., Rock, K.D., Belcher, S.M., 2024. Quantitative cross-species comparison of serum albumin binding of per-and polyfluoroalkyl substances from five structural classes. Toxicol Sci 199, 132–149. https://doi.org/10.1093/toxsci/kfae028.
[46] Fischer, F.C., Ludtke, S., Thackray, C., Pickard, H.M., Haque, F., Dassuncao, C., Endo, S., Schaider, L., Sunderland, E.M., 2024. Binding of per-and polyfluoroalkyl substances (PFAS) to serum proteins: implications for toxicokinetics in humans. Environ Sci Technol 58, 1055–1063. https://doi.org/10.1021/acs.est.3c07415.
[47] Perovani, I.S., Barbetta, M.F.S., Duarte, L.O., de Oliveira, A.R.M., 2023. Determination of polyfluoroalkyl substances in biological matrices by chromatography techniques: a review focused on the sample preparation techniques-Review. J Chromatogr Open 3, 100082. https://doi.org/10.1016/j.jcoa.2023.100082.
[48] Carignan, C.C., Bauer, R.A., Patterson, A., Phomsopha, T., Redman, E., Stapleton, H.M., Higgins, C.P., 2023. Self-collection blood test for PFASs: comparing volumetric microsamplers with a traditional serum approach. Environ Sci Technol 57, 7950–7957. https://doi.org/10.1021/acs.est.2c09852.
[49] Kaiser, A.M., Aro, R., Kärrman, A., Weiss, S., Hartmann, C., Uhl, M., Forsthuber, M., Gundacker, C., Yeung, L.W., 2021. Comparison of extraction methods for per-and polyfluoroalkyl substances (PFAS) in human serum and placenta samples—insights into extractable organic fluorine (EOF). Anal Bioanal Chem 413, 865–876. https://doi.org/10.1007/s00216-020-03041-5.
[50] Sanan, T., Magnuson, M., 2020. Analysis of per-and polyfluorinated alkyl substances in sub-sampled water matrices with online solid phase extraction/isotope dilution tandem mass spectrometry. J Chromatogr A 1626, 461324. https://doi.org/10.1016/j.chroma.2020.461324.
[51] McDonough, C.A., Choyke, S., Barton, K.E., Mass, S., Starling, A.P., Adgate, J.L., Higgins, C.P., 2021. Unsaturated PFOS and other PFASs in human serum and drinking water from an AFFF-impacted community. Environ Sci Technol 55, 8139–8148. https://doi.org/10.1021/acs.est.1c00522.
[52] Mancini, M., Gioia, V., Simonetti, F., Frugis, A., Cinti, S., 2023. Evaluation of pure PFAS decrease in controlled settings. ACS Meas Sci Au 3, 444–451. https://doi.org/10.1021/acsmeasuresciau.3c00027.
[53] Stecconi, T., Stramenga, A., Tavoloni, T., Bacchiocchi, S., Ciriaci, M., Griffoni, F., Palombo, P., Sagratini, G., Siracusa, M., Piersanti, A., 2024. Exploring perfluoroalkyl substances (PFASs) in aquatic fauna of lake Trasimeno (Italy): insights from a low-anthropized Area. Toxics 12, 196. https://doi.org/10.3390/toxics12030196.
[54] International Standard Organization/International Electro Technical Corporation (2017) ISO/IEC 17025: 2017—General requirements for the competence of testing and calibration laboratories.
[55] Yu, C., Stevenson, G., De Araujo, J., Crough, R., 2023. Application of in-source fragmentation to the identification of perfluoropentanoic acid and perfluorobutanoic acid in environmental matrices and human serum by isotope dilution liquid chromatography coupled with tandem mass spectrometry. Chemosphere 340, 139756. https://doi.org/10.1016/j.chemosphere.2023.139756.
[56] Hasegawa, K., Minakata, K., Suzuki, M., Suzuki, O., 2021. The standard addition method and its validation in forensic toxicology. Forensic Toxicol 39, 311–333. https://doi.org/10.1007/s11419-021-00585-8.
[57] Khan, I., Noor-ul-Amin, M., Khan, D.M., AlQahtani, S.A., Sumelka, W., 2023. Adaptive EWMA control chart using Bayesian approach under ranked set sampling schemes with application to Hard Bake process. Sci Rep 13, 9463. https://doi.org/10.1038/s41598-023-36469-7.